Pyramid Convolutional Network for Single Image Deraining

Jing Zhao
Peking University
Beijing, 100871, China
jzhaopku@pku.edu.cn

Jiyu Xie
University of Science and Technology
Hefei, 230026, China
xjy646@mail.ustc.edu.cn

Ruiqin Xiong
Peking University
Beijing, 100871, China
rqxiong@pku.edu.cn

Siwei Ma
Peking University
Beijing, 100871, China
swma@pku.edu.cn

Tiejun Huang
Peking University
Beijing, 100871, China
tjhuang@pku.edu.cn

Wen Gao
Peking University
Beijing, 100871, China
wgao@pku.edu.cn

Abstract

Restoring images corrupted by rain streaks is important for many computer vision applications in outdoor scenes. Benefiting from the fast inference and excellent feature representation capability, deep convolutional neural networks (CNN) have achieved significant performance improvement for image deraining and attracted considerable attention recently. However, for the images with complex background, the performance of these CNN-based methods is still unsatisfactory. Addressing this issue, we develop a new pyramid convolutional neural network, which is composed of multiple subnets, for image deraining, and name it PDRNet. To take full advantage of multi-scale redundancy, the network decomposes the rainy images into multi-scale subbands via a hierarchical wavelet transform and then process them by several sub-networks respectively. In particular, wavelet transform also plays the role of downsampling and enlarges the receptive field without increasing depth or sacrificing efficiency of network. Experimental results show that our PDRNet can not only achieve promising deraining performance quantitatively and qualitatively, but also benefit high-level computer vision tasks.

1. Introduction

Undesirable rain streaks are often presented in the images captured by outdoor equipments and heavily degrade the visual quality. Moreover, the effects of rain may also severely affect the performance of many outdoor computer vision applications, such as surveillance systems and unmanned cars. Thus, rain streak removal is an important problem and has attracted much research interest.

Image deraining is a ill-posed inverse problem and can be formulated as $Y = X + R$, where X is the background layer, R is the rain streak layer and Y is the image with rain streaks [13]. The goal of image deraining is to separate the background X from its corrupted observation Y. Over the past decades, many approaches have been proposed by exploring certain prior information on physical characteristics of rain streak [13, 10, 15, 2, 18]. Kang et al. [10] formulated rain removal as an image decomposition problem based on morphological component analysis. Luo et al. [15] exploited discriminative sparse coding model to solve the problem and Li et al. [13] developed a Gaussian mixture model to differentiate rain streaks and background images.

(a) (b)

Figure 1. An example of single image de-raining result on real-world image. (a) Real-world rainy image (b) Our result.

However, these models are generally based on hand-crafted priors, which may not be strong enough to characterize complex image structures. Recently, with the rapid development of deep networks, various powerful deep learning based methods have been proposed for image deraining [4, 3, 21, 12, 22, 17]. Some approaches [4, 3] focus on changing the mapping range from input to output for making the learning process easier. Some works are dedicated to exploring a multi-task network. Yang et al. [21] develope-

d a deep network to jointly detect and remove rain streaks. Zhang et al. [22] presented a CNN-based method for joint rain density estimation and de-raining.

Although considerable performance has been achieved by these learning-based methods, they are still weak in removing large rain streaks in complex background scenes and differentiating rain streaks from similar image textures of rain-free background. To address this issue, we develop a pyramid convolutional network which consists of multiple sub-networks of different scales. In order to fully exploit the multi-scale redundancy, we apply a hierarchical wavelet transform to decompose the rainy images into multi-scale subbands, and then forward them to corresponding sub-networks to remove rain streaks in different scales. For further improving feature representation capacity and restoring more image details, the network exploits coarse-to-fine restoration process by forwarding the features captured in lower sub-network to higher sub-network. Specially, wavelet transform can be regarded as a special downsampling which can enlarge the receptive field of network without increasing depth.

In summary, this paper makes the following contributions:

- We propose a pyramid convoluational neural network for single image deraining, named PDRNet. As shown in Fig. 1, benefiting from multi-scale redundancy and well-designed architecture, the PDRNet can promisingly remove rain streaks while preserving texture details.
- We adopt coarse-to-fine restoration process for better removing large rain streaks, which is generally more challenging.
- Considering that the process of deep network may incur the loss of information, we concatenate unprocessed signals with the the derained features periodically for recovering more details and further enhancing restoration performance.
- We evaluate our method on both synthetic and real datasets, and experimental results demonstrate that it can not only outperform the state-of-the-art methods quantitatively and qualitatively but also benefit high-level tasks.

2. Related Work

2.1. Single image deraining

Single image deraining is important for many outdoor computer vision applications, such as surveillance, pedestrian detection and autonomous driving, and has attracted widespread attention. Conventional approaches generally treated single image de-raining as a signal separation problem between rain streaks and rain-free background and solved the problem by exploiting certain prior knowledge, such as sparse representation [24], frenquany domain representation [10] and Gaussian mixture model [13]. However, because of the limitations of low-level hand-crafted priors, the performance of these methods is still unsatisfactory, especially for the images with complex textures.

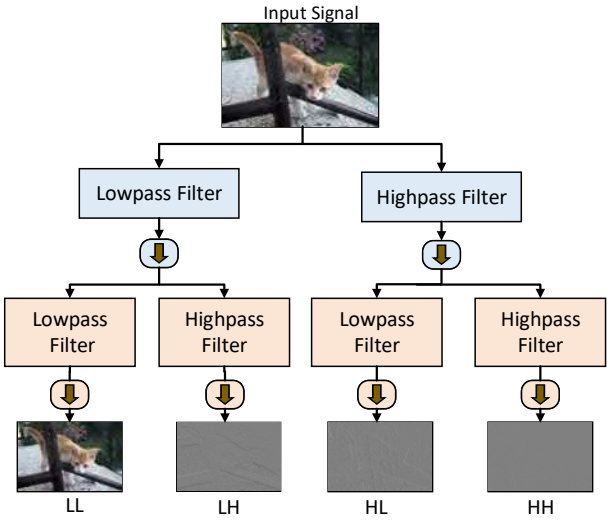

Figure 2. The diagram of 2-D discrete wavelet transform (DWT).

Recently, with the development of deep neural network, many learning based methods have been proposed for single image deraining. Fu et al. [3] presented a relative shallow network with 3 layers to remove rain from individual images. Inspired by ResNet [7], Fu et al. [4] further developed a deep detail network to learn residual with the high frequency information to improve the deraining performance. Yang et al. [21] proposed a deep recurrent network named JORDER to detect and remove rain streaks jointly. In [22] the authors presented a novel density aware multi-stream densely connected convolutional neural network, which can automatically determine the rain-density information and then efficiently remove the corresponding rain streaks. To fully exploit hierarchical features and further improve deraining performance, some methods [11, 20] introduced multi-scale model into the deraining network.

2.2. Wavelet transform based image processing

Over the past decades, wavelet transform has been widely applied in low-level image processing problems, such as super-resolution [23, 16], denoising [5] and deblocking [8]. Recently, some works proposed to combine the benefit of wavelet transform with the potential deep neural network. In [1], a one-layer wavelet transform was adopted to simplify the topological structures of network's input. In [14], a multi-level wavelet based CNN architecture was developed for image restoration and achieved better trade-off between

receptive field size and computational efficiency. Yang et al. [20] embed a hierarchical representation of wavelet transform into a recurrent rain removal process. Compared to [20], our PDRNet combines original rainy images with derained features for more details, and adopts muli-scale loss function to mimic coarse-to-fine restoration process.

3. Method

In this section, we first introduce the multi-level wavelet transform. Subsequently, we present our pyramid convolutional network, which consists of multiple subnets with different scales, and then describe its network architecture and multi-scale loss.

3.1. Multi-level wavelet decomposition

Our method is built on 2-D discrete wavelet transform (DWT) to take the advantage of spatial-frequency localization. As shown in Fig. 2, the 2-D wavelet decomposition is performed by first applying 1-D DWT along the rows of the input image I, and then decomposing the acquired results along the columns. As a result, there are four subbands referred to low-low (LL), low-high (LH), high-low (HL), and high-high (HH), where the L-L subband can be regarded as the approximation component of the image, while the other subbands can be regarded as the detailed components of the image. The procedure of 2-D wavelet decomposition is formulated as $[LL, LH, HL, HH] = \text{DWT}(I)$, while the inverse operation is formulated as $I = \text{IDWT}([LL, LH, HL, HH])$.

Specially, for fully exploiting multi-scale redundancy and well removing all levels of rain streaks, this paper adopts a multi-level wavelet transform to decompose rainy images into hierarchical subbands: the one-level 2-D wavelet transform first decompose the image into four subbands. Then, the two-level DWT decompose the low-frequency component into four subbands and get four two-level subbands. Recursively, the results of three or higher level DWT can be attained.

We note that applying the multi-level DWT to our network has the following advantages. Firstly, the DWT can be regarded as a special downsampling, and multi-level DWT can effectively enlarge the receptive field of network without increasing depth or sacrificing efficiency. Moreover, the size of rain streaks presents strong diversity and the removal of large rain streaks is usually intractable. With the aid of multi-level DWT decomposition, the network first shrinks the signals in lower scales, which makes removing the large rain streaks easier.

3.2. Proposed pyramid convolutional network

Suppose $\{Y_0, X_0\}$ is the rain and rain-free image pair. In this paper, we adopt a two-level wavelet transform to decompose the image into a over-complete hierarchical representation, so we have:

$$\begin{aligned}[Y_1^{\text{LL}}, Y_1^{\text{LH}}, Y_1^{\text{HL}}, Y_1^{\text{HH}}] &= \text{DWT}(Y_0),\\ [Y_2^{\text{LL}}, Y_2^{\text{LH}}, Y_2^{\text{HL}}, Y_2^{\text{HH}}] &= \text{DWT}(Y_1^{\text{LL}}),\end{aligned} \tag{1}$$

where $[Y_1^{\text{LL}}, Y_1^{\text{LH}}, Y_1^{\text{HL}}, Y_1^{\text{HH}}]$ are the one-level subbands and $[Y_2^{\text{LL}}, Y_2^{\text{LH}}, Y_2^{\text{HL}}, Y_2^{\text{HH}}]$ are the subbands after two-level wavelet transform.

As shown in Fig. 3, the proposed network is composed of three sub-networks with different scales and utilizes coarse-to-fine architecture. The network first processes the coarsest subbband, which is decomposed by two-level DWT, to capture the long-range dependencies and then exploits the finer scale sub-networks to restore more details.

Let F_2 denotes the coarsest sub-network. Based on the assumption that the residual mapping is much easier to be learned than the original unreferenced one, we adopts residual learning strategy, and the derained subband of the coarsest scale is denoted as

$$\hat{X}_2^{\text{LL}} = F_2(Y_2^{\text{LL}}) + Y_2^{\text{LL}}. \tag{2}$$

Subsequently, we use zeros to pad other frequency components (LH, HL, HH) and apply an inverse discrete wavelet transform (IDWT) on these subbands as upsampling for

$$\widetilde{X}_1^{\text{LL}} = H(\hat{X}_2^{\text{LL}}) = \text{IDWT}(\hat{X}_2^{\text{LL}}, \mathbf{0}, \mathbf{0}, \mathbf{0}), \tag{3}$$

so that we can integrate the features of coarsest scale with the finer ones. Then, the fused signals are forwarded into the second sub-network F_1 for corresponding derained subband

$$\hat{X}_1^{\text{LL}} = F_1([Y_1^{\text{LL}}, \widetilde{X}_1^{\text{LL}}]) + Y_1^{\text{LL}}, \tag{4}$$

where $[Y_1^{\text{LL}}, \widetilde{X}_1^{\text{LL}}]$ represents the concatenation of the rainy subband of the corresponding scale and the image reconstructed from the former sub-network' output.

Similarly, we perform an IDWT on $\hat{X}_1^{\text{LL}}$ to get

$$\widetilde{X}_0^{\text{LL}} = H(\hat{X}_1^{\text{LL}}) = \text{IDWT}(\hat{X}_1^{\text{LL}}, \mathbf{0}, \mathbf{0.0}), \tag{5}$$

and forward the obtained features and the original rainy image to the third sub-network F_0 for final derained image

$$\hat{X}_0 = F_0([Y_0, \widetilde{X}_0^{\text{LL}}]) + Y_0. \tag{6}$$

Fig. 3 shows the architecture of the proposed network. We use color to differentiate varieties of layers. Inspired by the potential ResNet [7], our network is based on residual blocks. Each residual block consists of one residual connection, one parameteric rectified linear unit (PReLU), two "Conv+BN+PReLU" layers and one "Conv+BN" layer, in which bypass connection is conducted by elementwise

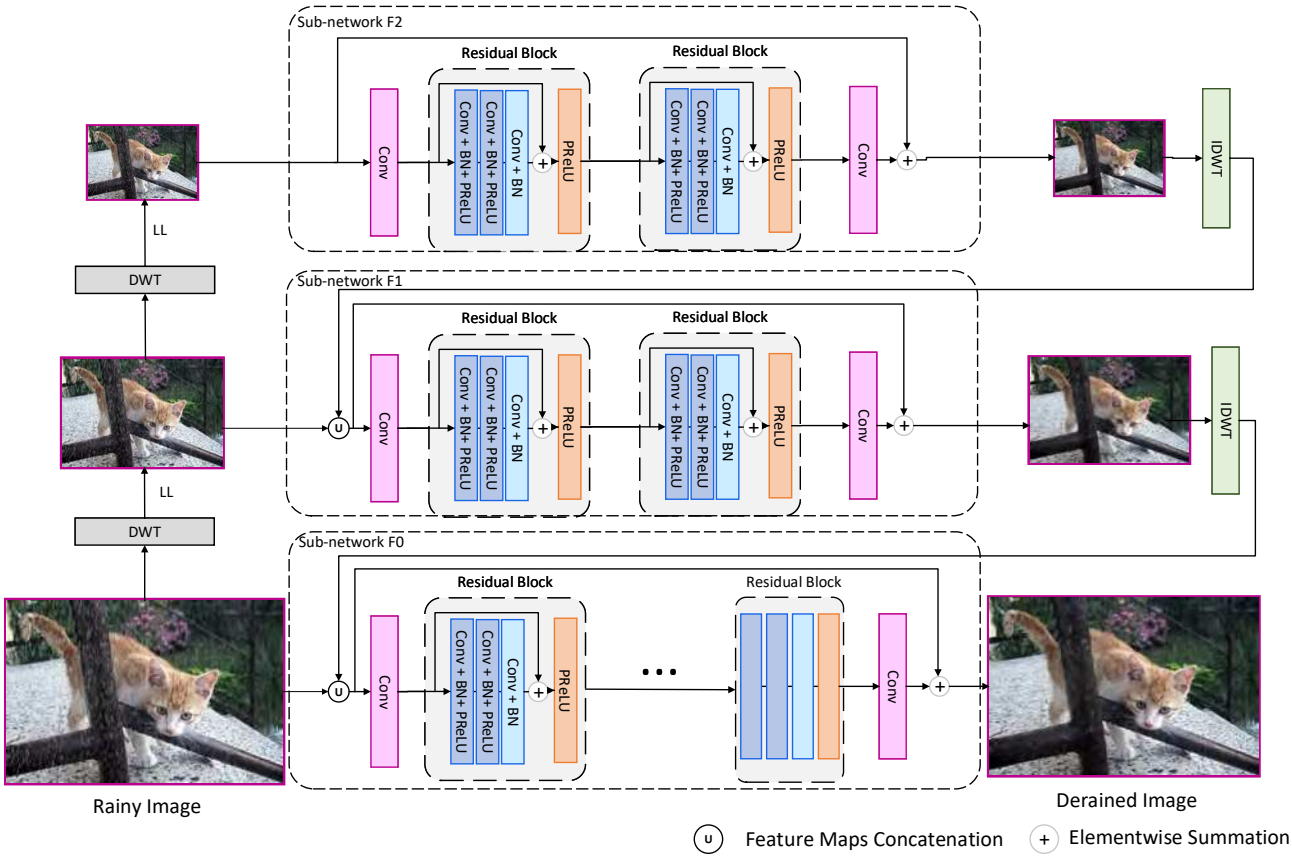

Figure 3. The architecture of the proposed PDRNet.

summation for alleviating gradient vanishing problem. Specially, in order to enrich feature representation and forward more details, we add feature maps concatenation at the front of each sub-network to integrate the derained features of coarser scale to the finer subbands. The network configuration details are presented in Table 1, where h and w depend on the size of the image to derain.

3.3. Multi-scale loss function

We propose a multi-scale loss to direct the network's training so that the reconstructed image can retain both small details on finer scales and long-range dependencies on coarser scales. Given the set of rainy-clean pairs $S = \{(\boldsymbol{Y}_0; \boldsymbol{X}_0)\}$, where $\boldsymbol{Y}_0(i)$ is the ith image to derain and $\boldsymbol{X}_0(i)$ represents the corresponding ground-truth image, the loss function is defined as:

$$\begin{aligned}\mathcal{L}(\Theta) = \frac{1}{2N}\sum_{i=1}^{N}\Big(&\alpha\left\|\boldsymbol{X}_2^{\mathrm{LL}}(i) - \hat{\boldsymbol{X}}_2^{\mathrm{LL}}(i)\right\|_F^2 \\ &+ \beta\left\|\boldsymbol{X}_1^{\mathrm{LL}}(i) - \hat{\boldsymbol{X}}_1^{\mathrm{LL}}(i)\right\|_F^2 \\ &+ \gamma\left\|\boldsymbol{X}_0^{\mathrm{LL}}(i) - \hat{\boldsymbol{X}}_0^{\mathrm{LL}}(i)\right\|_F^2.\end{aligned} \tag{7}$$

Here $\boldsymbol{X}_1^{\mathrm{LL}}(i)$, $\boldsymbol{X}_2^{\mathrm{LL}}(i)$ are the subbands obtained from ground-truth $\boldsymbol{X}_0^{\mathrm{LL}}(i)$ via DWT. $\hat{\boldsymbol{X}}_0^{\mathrm{LL}}(i)$, $\hat{\boldsymbol{X}}_1^{\mathrm{LL}}(i)$ and $\hat{\boldsymbol{X}}_2^{\mathrm{LL}}(i)$ are the outputs of corresponding sub-networks when deraining $\boldsymbol{Y_0}(i)$, and Θ is the set of network parameters. α, β and γ are the weights for different scales and the weight γ for the final image is generally bigger than the others. In this paper, they are empirically set to 0.5, 0.5 and 1, respectively.

4. Experimental Results

4.1. Datasets and evaluation criteria

We evaluate the performance of our proposed PDRNet on both synthetic and real-world data. For synthetic data, we use two benchmark datasets: 1) $Rain100L$ [21]: There are 1800 images for training plus 100 images for testing. In $Rain100L$, the rainy images are synthesized with only one type of rain streaks. 2) $Rain100H$ [21]: Compared to $Rain100L$, it is more challenging, which is synthesized by large rain streaks with five directions. As $Rain100L$, it also includes 1800 images for training and 100 images for testing. For real-world data, some of them are collected from the Internet and some are from the released images of

Table 1. Detailed configuration of PDRNet.

Sub-Network	Layer	Kernerl Size	Filter Number	Input Size	Output Size
Sub-network1	Conv	3×3	128	h/4 × w/4	h/4 × w/4
	Residual Block	$\begin{bmatrix} 3 \times 3 \\ 3 \times 3 \\ 3 \times 3 \end{bmatrix}$	128	h/4 × w/4	h/4 × w/4
	Residual Block	$\begin{bmatrix} 3 \times 3 \\ 3 \times 3 \\ 3 \times 3 \end{bmatrix}$	128	h/4 × w/4	h/4 × w/4
	Conv	3×3	3	h/4 × w/4	h/4 × w/4
	Inverse DWT	-	-	h/4 × w/4	h/2 × w/2
Sub-network2	Conv	3×3	128	h/2 × w/2	h/2 × w/2
	Residual Block	$\begin{bmatrix} 3 \times 3 \\ 3 \times 3 \\ 3 \times 3 \end{bmatrix}$	128	h/2 × w/2	h/2 × w/2
	Residual Block	$\begin{bmatrix} 3 \times 3 \\ 3 \times 3 \\ 3 \times 3 \end{bmatrix}$	128	h/2 × w/2	h/2 × w/2
	Conv	3×3	3	h/2 × w/2	h/2 × w/2
	Inverse DWT	-	-	h/2 × w/2	h × w
Sub-network3	Conv	3×3	128	h × w	h × w
	Residual Block	$\begin{bmatrix} 3 \times 3 \\ 3 \times 3 \\ 3 \times 3 \end{bmatrix}$	128	h × w	h × w
	Residual Block	$\begin{bmatrix} 3 \times 3 \\ 3 \times 3 \\ 3 \times 3 \end{bmatrix}$	128	h × w	h × w
	Residual Block	$\begin{bmatrix} 3 \times 3 \\ 3 \times 3 \\ 3 \times 3 \end{bmatrix}$	128	h × w	h × w
	Residual Block	$\begin{bmatrix} 3 \times 3 \\ 3 \times 3 \\ 3 \times 3 \end{bmatrix}$	128	h × w	h × w
	Conv	3×3	3	h × w	h × w

[22] and [21].

For the experiments on synthesized data, two metrics Peak Signal-to-Noise Ratio (PSNR) [9] and Structure Similarity Index (SSIM) [19] are used to evaluate the performance. Following the existing works [22, 21], we only evaluate the results in the luminance channel, which has the most significant impact on the human visual system. Since the rain-free ground-truth of real-world images are not available, we only use visual results to compare the performance of real-world data.

4.2. Implementation

We set patch size as 120×120 and batch size as 24. Before training network, the rainy-clean patch pairs are transformed into multi-level subbands. The loss function in Eqn. (7) is adopted to train the mapping from rainy images to the clean ones. We initialize the weights by the method in [6] and use ADAM algorithm with the default setting to optimize our network. The learning rate is decayed exponentially from 2×10^{-4} to 2×10^{-6}.

The network is implemented on Pytorch 0.4.1 environment running on a machine with Intel(R) Xeon(R) E5-

Table 2. Average PSNR(dB)/SSIM results of different methods for single image deraining on datasets $Rain100L$ and $Rain100H$. We highlight the best two results in red and blue respectively.

Dataset	Metric	DSC [15]	GMM [13]	DDN [4]	JORDER [21]	DID-MDN [22]	PDRNet
$Rain100L$	*PSNR*	27.40	28.66	29.36	35.92	30.48	36.30
	SSIM	0.8543	0.8653	0.9211	0.9712	0.9323	0.9767
$Rain100H$	*PSNR*	14.31	15.05	16.02	25.48	26.35	26.94
	SSIM	0.3620	0.4252	0.6398	0.8134	0.8287	0.8577

Figure 4. Visual comparison of our PDRNet with state-of-the-art rain removal algorithms on synthetic rain images. From left to right: the rainy inputs, derained images by DSC, derained images by DDN, derained images by JORDER, derained images by our PDRNet and ground-truth. We can observe that our method performs better on restoring details. Please enlarge the figure for more details.

Figure 5. Visual comparison of our PDRNet with state-of-the-art rain removal algorithms on real-world images. From left to right: the rainy inputs, derained images by DSC, derained images by DDN, derained images by JORDER, and the derained images by our PDRNet. We can observe that our method achieves the best visualization results. Please enlarge the figure for more details.

2630 CPU 2.40GHz and an Nvidia TITAN Xp GPU. It takes about 1.5 days for training a deraining model on the $Rain100H$ or $Rain100L$ training dataset.

4.3. Comparison with the state-of-the-art

To evaluate the performance of the proposed PDRNet, we compare our method with five state-of-the-art single-

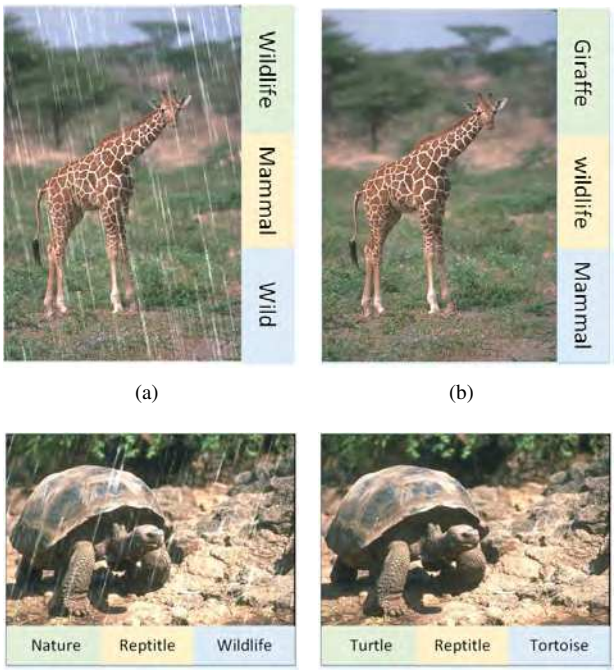

(a) (b) (c) (d)

Figure 6. Image recognition results on the images before and after rain streak removal. (a) Result on rainy image, labelled as wildlife. (b) Result on our derained image, labelled as giraffe. (c) Result on rainy image, labelled as Nature (d) Result on our derained image, labelled as turtle.

image de-raining methods, including discriminative sparse coding (DSC) [15], GMM-based layer prior (GMM) [13], deep detail network (DDN) [4], joint rain detection and removal (JORDER) [21] and density-aware multi-stream dense network (DID-MDN) [22]. For fair comparision, two models, one for $Rain100H$ and one for $Rain100L$, are trained for each deep learning based method.

Quantitative Evaluation. Table 2 lists the PSNR and SSIM results of different methods on two synthetic datasets. We note that our proposed PDRNet achieves considerable performance in terms of both PSNR and SSIM. In particular, for the challenging dataset $Rain100H$ with large rain streaks of various directions, our PDRNet outperforms the competitive methods JORDER and DID-MDN by about 1.5dB and 0.6dB respectively, while other methods perform unsatisfactory.

Qualitative Evaluation. Fig. 4 shows visual comparisons of rain-streaks removal results on synthesized rainy images. Fig. 5 presents the results of some real images. As can be observed, our proposed method shows the best visual performance on rain-streaks removal, which can not only recover sharp textures and fine details but also produce promising perceptual quality in the smooth region.

4.4. Application in computer vision

The effects of rain streaks may heavily affect the performance of many computer vision applications. Specially, our method can be used as preprocessing to improve the performance of computer vision applications under rainy scenes. Fig .6 shows two cases of applying our method as preprocessing for an advanced image recognition system, i.e. Clarifai [1]. We display the top three recognition results, where green represents the most probable label and yellow takes the second place. As can be observed, compared to direct recognition on the rainy images, the preprocessing can improve the recognition accuracy. Before rain removal, these images are roughly categorized as "Wildlife" and "Nature". After preprocessed by our PDRNet, they are labelled accurately as "Giraffe" and "turtle", respectively.

5. Conclusion

In this paper, we develop a new pyramid convolutional network for single image deraining, named PDRNet. A hierarchical wavelet transform is adopted to decompose images into several subbands with different scales for fully exploiting the multi-scale redundancy so that the PDRNet is more effective in removing rain streaks from complex background. Moreover, the wavelet transform works as a downsampling operator with better tradeoff between efficiency and performance by enlarging the receptive field of network without increasing depth. Experimental results demonstrate that our method achieves competitive deraining performance and is beneficial to computer vision applications.

Acknowledgements

This work was supported in part by the National Key Research and Development Program of China(2017YFB1002203), the National Basic Research Program of China (2015CB351800) and the National Natural Science Foundation of China (61772041).

References

[1] Woong Bae, Jaejun Yoo, and Jong Chul Ye. Beyond deep residual learning for image restoration: Persistent homology-guided manifold simplification. In *Proceedings of the IEEE Conference on Computer Vision and Pattern Recognition Workshops*, pages 145–153, 2017.

[2] Yi-Lei Chen and Chiou-Ting Hsu. A generalized low-rank appearance model for spatio-temporally correlated rain streaks. In *Proceedings of the IEEE International Conference on Computer Vision*, pages 1968–1975, 2013.

[3] Xueyang Fu, Jiabin Huang, Xinghao Ding, Yinghao Liao, and John Paisley. Clearing the skies: A deep network archi-

[1] https://www.clarifai.com/.

tecture for single-image rain removal. *IEEE Transactions on Image Processing*, 26(6):2944–2956, 2017.

[4] Xueyang Fu, Jiabin Huang, Delu Zeng, Yue Huang, Xinghao Ding, and John Paisley. Removing rain from single images via a deep detail network. In *Proceedings of the IEEE Conference on Computer Vision and Pattern Recognition*, pages 3855–3863, 2017.

[5] Vikas Gupta, Rajesh Mahle, and Raviprakash S Shriwas. Image denoising using wavelet transform method. In *2013 Tenth International Conference on Wireless and Optical Communications Networks (WOCN)*, pages 1–4. IEEE, 2013.

[6] Kaiming He, Xiangyu Zhang, Shaoqing Ren, and Jian Sun. Delving deep into rectifiers: Surpassing human-level performance on imagenet classification. In *Proceedings of the IEEE international conference on computer vision*, pages 1026–1034, 2015.

[7] Kaiming He, Xiangyu Zhang, Shaoqing Ren, and Jian Sun. Deep residual learning for image recognition. In *Proceedings of the IEEE conference on computer vision and pattern recognition*, pages 770–778, 2016.

[8] Tai-Chiu Hsung, D Pak-Kong Lun, and Wan-Chi Siu. A deblocking technique for block-transform compressed image using wavelet transform modulus maxima. *IEEE transactions on image processing*, 7(10):1488–1496, 1998.

[9] Quan Huynh-Thu and Mohammed Ghanbari. Scope of validity of psnr in image/video quality assessment. *Electronics letters*, 44(13):800–801, 2008.

[10] Li-Wei Kang, Chia-Wen Lin, and Yu-Hsiang Fu. Automatic single-image-based rain streaks removal via image decomposition. *IEEE Transactions on Image Processing*, 21(4):1742–1755, 2012.

[11] Guanbin Li, He Xiang, Zhang Wei, Huiyou Chang, and Lin Liang. Non-locally enhanced encoder-decoder network for single image de-raining. 2018.

[12] Ruoteng Li, Loong-Fah Cheong, and Robby T Tan. Single image deraining using scale-aware multi-stage recurrent network. *arXiv preprint arXiv:1712.06830*, 2017.

[13] Yu Li, Robby T Tan, Xiaojie Guo, Jiangbo Lu, and Michael S Brown. Rain streak removal using layer priors. In *Proceedings of the IEEE conference on computer vision and pattern recognition*, pages 2736–2744, 2016.

[14] Pengju Liu, Hongzhi Zhang, Kai Zhang, Liang Lin, and Wangmeng Zuo. Multi-level wavelet-cnn for image restoration. In *Proceedings of the IEEE Conference on Computer Vision and Pattern Recognition Workshops*, pages 773–782, 2018.

[15] Yu Luo, Yong Xu, and Hui Ji. Removing rain from a single image via discriminative sparse coding. In *Proceedings of the IEEE International Conference on Computer Vision*, pages 3397–3405, 2015.

[16] Sapan Naik and Nikunj Patel. Single image super resolution in spatial and wavelet domain. *arXiv preprint arXiv:1309.2057*, 2013.

[17] Rui Qian, Robby T Tan, Wenhan Yang, Jiajun Su, and Jiaying Liu. Attentive generative adversarial network for raindrop removal from a single image. In *Proceedings of the IEEE Conference on Computer Vision and Pattern Recognition*, pages 2482–2491, 2018.

[18] Shao-Hua Sun, Shang-Pu Fan, and Yu-Chiang Frank Wang. Exploiting image structural similarity for single image rain removal. In *2014 IEEE International Conference on Image Processing (ICIP)*, pages 4482–4486. IEEE, 2014.

[19] Zhou Wang, Alan C Bovik, Hamid R Sheikh, Eero P Simoncelli, et al. Image quality assessment: from error visibility to structural similarity. *IEEE transactions on image processing*, 13(4):600–612, 2004.

[20] Wenhan Yang, Jiaying Liu, Shuai Yang, and Zongming Guo. Scale-free single image deraining via visibility-enhanced recurrent wavelet learning. *IEEE Transactions on Image Processing*, 28(6):2948–2961, 2019.

[21] Wenhan Yang, Robby T Tan, Jiashi Feng, Jiaying Liu, Zongming Guo, and Shuicheng Yan. Deep joint rain detection and removal from a single image. In *Proceedings of the IEEE Conference on Computer Vision and Pattern Recognition*, pages 1357–1366, 2017.

[22] He Zhang and Vishal M Patel. Density-aware single image de-raining using a multi-stream dense network. In *Proceedings of the IEEE Conference on Computer Vision and Pattern Recognition*, pages 695–704, 2018.

[23] Shubin Zhao, Hua Han, and Silong Peng. Wavelet-domain hmt-based image super-resolution. In *Proceedings 2003 International Conference on Image Processing (Cat. No. 03CH37429)*, volume 2, pages II–953. IEEE, 2003.

[24] Lei Zhu, Chi-Wing Fu, Dani Lischinski, and Pheng-Ann Heng. Joint bi-layer optimization for single-image rain streak removal. In *Proceedings of the IEEE international conference on computer vision*, pages 2526–2534, 2017.